

## Fermi surface of $\text{LaFe}_2\text{P}_2$ —a detailed density functional study

Förster, T.; Kraft, I.; Sheikin, I.; Bianchi, A. D.; Wosnitza, J.; Rosner, H.;

Originally published:

October 2019

**Journal of Physics: Condensed Matter 32(2020), 025503**

DOI: <https://doi.org/10.1088/1361-648X/ab45fa>

Perma-Link to Publication Repository of HZDR:

<https://www.hzdr.de/publications/Publ-29891>

Release of the secondary publication  
on the basis of the German Copyright Law § 38 Section 4.

# Fermi surface of $\text{LaFe}_2\text{P}_2$ - a detailed Density Functional study

T. Förster<sup>1</sup>, I. Kraft<sup>2</sup>, I. Sheikin<sup>3</sup>, A. D. Bianchi<sup>4</sup>, J. Wosnitza<sup>1,5</sup> and H. Rosner<sup>2</sup>

<sup>1</sup> Hochfeld-Magnetlabor Dresden (HLD-EMFL), Helmholtz-Zentrum Dresden-Rossendorf, D-01314 Dresden, Germany

<sup>2</sup> Max Planck Institute for Chemical Physics of Solids, 01187 Dresden, Germany

<sup>3</sup> Laboratoire National des Champs Magnétiques Intenses (LNCMI), CNRS, UJF, 38042 Grenoble, France

<sup>4</sup> Département de Physique and RQMP, Université de Montréal, Montréal H3C 3J7, Canada

<sup>5</sup> Institut für Festkörperphysik, TU Dresden, D-01062 Dresden, Germany

**Abstract.** Angular dependent de Haas-van Alphen measurements allow to map Fermi surfaces in great detail with high accuracy. Density functional electronic structure calculations can be carried out with high precision, but depend crucially on the used structural information and the applied calculational approximations. We report in a detailed study about the sensitivity of the calculated electronic band structure of the 122 compound  $\text{LaFe}_2\text{P}_2$  on (i) the exact P position in the unit cell, parametrized by a so-called  $z$  parameter, and on (ii) the treatment of the La  $4f$ -states. Depending on the chosen exchange and correlation-potential approximation, the calculated  $z$  parameter varies slightly and corresponding small but distinctive differences in the calculated band structure and Fermi-surface topology appear. Similarly, topology changes appear when the energy of the mostly unoccupied La  $4f$ -states is corrected regarding their experimentally observed position. The calculated results are compared to experimental de Haas-van Alphen data. Our findings show a high sensitivity of the calculated band structure on the pnictide  $z$  position and the need for an accurate experimental determination of this parameter at low temperatures, and in particular the need of a sophisticated treatment of the La  $4f$ -states. Thus, this is not only crucial for the special case of  $\text{LaFe}_2\text{P}_2$  studied here, but of importance for the precise determination of the band structure of related 122 materials and La containing compounds in general.

PACS numbers: 1234,4321

Submitted to: *J. Phys.: Condens. Matter*

## 1. Introduction

The comprehensive and detailed knowledge of the electronic band structure is a necessary ingredient for the fundamental understanding of the physical properties of solids. To date, a number of powerful state-of-the-art software packages are on the market that allow to calculate the band structures and Fermi surfaces of metals with high a precision and give essentially the same result. But the unknown part of the interaction energy, the exchange-correlation functional and its specific implementation in the codes gives rise to small differences in the result of these complex numerical problems [40]. So, only the experiment can decide on the validity of the outcome of such calculations. One of the most powerful bulk methods to experimentally determine Fermi-surface parameters is to measure magnetic-field-induced quantum oscillations in, e.g., the magnetization [de Haas-van Alphen (dHvA) effect] or the resistance [Shubnikov-de Haas (SdH) effect] [1]. These techniques provide not only very accurate values for the extremal Fermi-surface cross sections, but also the corresponding renormalized effective masses and quasiparticle scattering rates.

Soon after the discovery of superconductivity in quaternary oxypnictides [2, 3] and the iron-pnictides [4] first band-structure calculations appeared [5, 6, 7, 8, 9, 10]. The predicted peculiar Fermi-surface topology, in turn, stimulated a number of theories on the nature of superconducting pairing in these materials [9, 10, 11, 12, 13, 14, 15, 16]. These theories are based on the nesting between the electron and hole bands of the quasi-two-dimensional Fermi-surface sheets. Unconventional superconductivity might result from interband scattering leading to an extended  $s$ -wave pairing,

with the superconducting gap changing signs between the hole and electron Fermi surfaces.

Experimental support for the band-structure calculations was first given by angular resolved photoemission spectroscopy (ARPES) [17, 18] and later by dHvA or SdH studies [19, 20, 21, 22, 23, 24, 25, 26]. In the latter experiments, besides some oxypnictides [19, 20, 21], mainly 122 iron pnictides ( $X\text{Fe}_2\text{As}_2$  and  $X\text{Fe}_2\text{P}_2$ , with  $X = \text{Sr}, \text{Ca}, \text{Ba}$ ) were investigated (see Refs. [27, 28] for reviews). All these data are in reasonable agreement with the predicted band structure. Most importantly, two electron and two hole quasi-two-dimensional Fermi-surface sheets can be assigned in the superconducting  $\text{LaFePO}$  [19, 20]. This supports the already mentioned notion of Cooper pairing due to interband scattering. There are, however, some examples where deviations from the band-structure predictions were observed in experiments, which are thought to be important for understanding the nature of the electronic properties in these materials, i.e. for the occurrence and stability of either superconductivity, and/or magnetic order. Such an example is  $\text{SrFe}_2\text{P}_2$ , a non-superconducting phosphide analogue of the 122 iron-arsenide materials, for which some discrepancies between experiment and calculation were reported [25]. Also here, two hole and electron sheets can be resolved. The corrugation of the Fermi-surface cylinders is, as generally found for the 122 materials, much more pronounced than for the superconducting oxypnictides. Thus, the Fermi-surface sheets in  $\text{SrFe}_2\text{P}_2$  do not fulfill a nesting condition. Indeed, neither superconductivity nor magnetic order has been observed in  $\text{SrFe}_2\text{P}_2$ .

Here, we report on comprehensive band-structure calculations for the isostructural

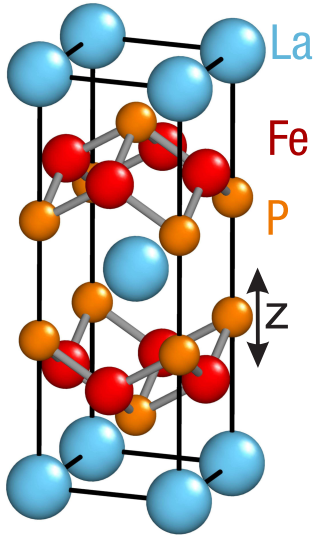


**Figure 1.** Crystal structure of  $\text{LaFe}_2\text{P}_2$  (space group  $I4/mmm$ ). The black arrow marks the only degree of freedom, the  $z$  parameter of the P (4e) position.

122 iron phosphide  $\text{LaFe}_2\text{P}_2$ , replacing the divalent Sr by the trivalent rare earth metal La.  $\text{LaFe}_2\text{P}_2$  shows no signs of magnetic or superconducting order down to 20 mK [31]. When comparing the calculated extremal Fermi-surface orbits with experimental data, we realized a high sensitivity of the computed results on the exact P position within the tetragonal crystal structure (Fig. 1). The calculated Fermi surface and the density of states at the Fermi energy change significantly when allowing the P position (reflected by the distance  $z$  of the P atom from the basal plane) to relax and depending on the used exchange and correlation potential  $V_{xc}$ . This holds true for other 122 compounds as well.

Indeed, in the 122 systems the Fe-pnictide inter layer distance is smaller than in other pnictides making the interlayer-interaction strongly depended on the  $c$  lattice parameter and the internal  $z$  position.

This results in a strong dependence of the electronic structure near the Fermi level

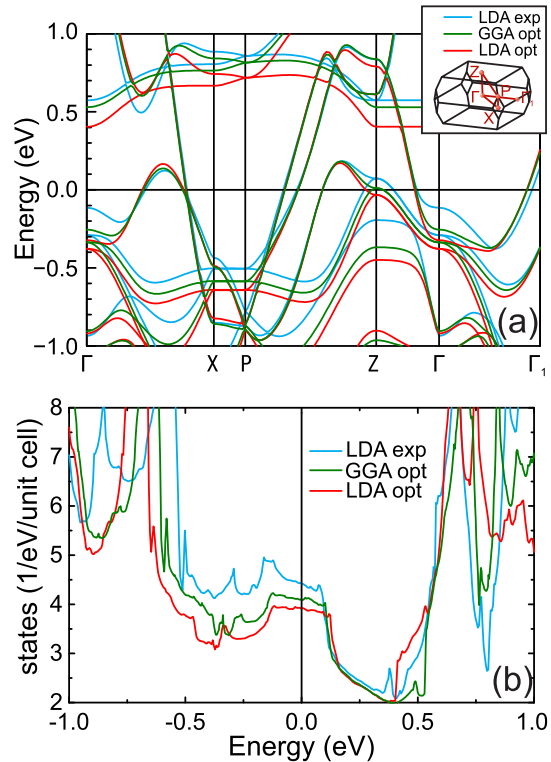


**Figure 2.** Band structure (a) and density of states (b) of  $\text{LaFe}_2\text{P}_2$ . The colors depict calculations with different  $z$  parameter of the P (4e) position: (blue) experimentally determined  $z = 0.3557$  [35], (green) optimized applying GGA yielding  $z = 0.3505$ , and (red) alternatively optimized applying LDA resulting in  $z = 0.3477$ . The inset in (a) shows the Brillouin zone with some symmetry points.

on the interlayer coupling and can lead to isostructural phase transitions under applied hydrostatic pressure such as the tetragonal collapsed phase in  $\text{CaFe}_2\text{As}_2$  [29] or  $\text{SrFe}_2\text{As}_2$  [30].

## 2. Method

The band structure was calculated using the full potential local-orbital (FPLO 9.01-35) [32] code on a well converged  $24 \times 24 \times 24$   $k$  mesh. Exchange and correlation potentials were estimated using either the local density approximation (LDA) [33] or generalized gradient approximation (GGA)



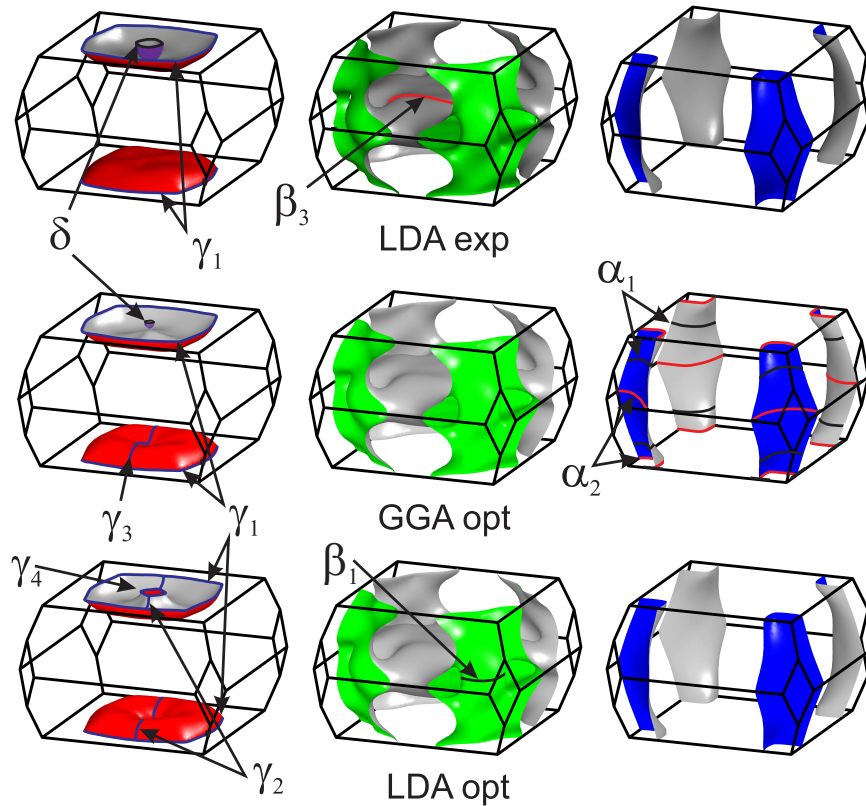


**Figure 3.** Calculated Fermi surfaces of  $\text{LaFe}_2\text{P}_2$  estimated with different  $z$  parameters as explained in Fig. 2. (upper panel) Experimentally determined  $z = 0.3557$  [35], (middle panel) optimized applying GGA ( $z = 0.3505$ ), and (lower panel) optimized applying LDA ( $z = 0.3477$ ). Some of the dHvA orbits are depicted by solid lines and labeled (see Fig. 4).

[34]. Treatments of the La  $4f$  states, which in LDA approximation lie too close to the Fermi energy,  $E_F$ , will be discussed below. As a starting point, we used the structural data obtained at room temperature by [35]:  $a = 3.8382(9)$  Å  $c = 11.006(6)$  Å  $z = 0.3557$ .

We compare our results with experimental dHvA data measured by use of torque magnetometers [31]. For that, we used CuBe capacitive cantilevers fixed on platforms that could be rotated *in situ* around one axis. Placing the sample on these cantilevers, the dHvA effect is measured as field-dependent oscillations of the capacitance. The measurements were performed at the Dresden High Magnetic Field Laboratory (HLD) in a superconducting 20-T magnet and at the Grenoble High Magnetic

Field Laboratory (LNCMI-Grenoble) using a resistive magnet in fields up to 34 T [31].

### 3. Results and discussion

We first consider the high sensitivity of the band structure and the density of states (DOS) on the position  $z$  of the P atom. Figure 2 shows the calculated band structure and DOS close to the Fermi level for  $\text{LaFe}_2\text{P}_2$ . Starting with the experimentally determined room-temperature P position, with  $z = 0.3557$  as the relative  $c$ -axis unit-cell parameter, and the LDA the blue curves are calculated (Fig. 2). When using instead GGA potentials with the same fixed  $z$ , virtually the same band structure is obtained (data not shown). Indeed, for any fixed  $z$  LDA

and GGA result in practically identical band structures.

Although the  $z$  position at room temperature is well defined, it may change upon cooling. We, therefore, allowed the P to relax to its optimum position by minimizing the total energy within the used potential approximation. Interestingly, clearly different  $z$  resulted when using either GGA ( $z = 0.3505$ ) or LDA ( $z = 0.3477$ ), with the clear trend towards somewhat smaller  $z$  positions, i.e., 1 – 2 % smaller than the experimental value. It is worth to note that this difference is several times larger than the difference in  $z$  observed by cooling  $\text{SrCo}_2\text{P}_2$  from room temperature down to 10 K [43]. The reduction of  $z$  also reduces the distance between Fe and P by 0.04 Å. This leads to substantial modifications of the band structure and the DOS (Fig. 2). The largest changes appear at the  $Z$  point of the Brillouin zone, where some bands below  $E_F$  shift down by up to 0.3 eV and another band is pushed below  $E_F$  when  $z$  is the smallest (red curve for LDA opt).

In consequence, this leads to a considerable reduction of the DOS at  $E_F$  [(Fig. 2(b)] and even to a change of the Fermi-surface topology (Fig. 3). For large  $z$ , i.e., for the experimental P position, two Fermi-surface sheets appear around  $Z$ , one pillow-like (shown in red in Fig. 3) and one small spherical sheet (purple). With decreasing  $z$ , the spherical sheet first becomes tiny (for GGA opt) and eventually vanishes for LDA opt. At the same time, the pillow develops a hole around  $Z$  leading to a donut-like shape. The other two sheets (green and blue sheets in Fig. 3) only change their sizes but keep their topologies.

For a comparison with the experimental dHvA data we need to determine the extremal Fermi-surface cross sections perpendicular to the applied magnetic fields. Such extremal

orbits for fields along [001] and [100] are marked by solid lines in Fig. 3 and labeled by different Greek letters for the different Fermi-surface sheets. Calculating these orbits for various angles within the main rotation planes, we can compare the result with our dHvA data, as shown in Fig. 4. The overall agreement between the calculations and experiment is very good, but there are some modifications appearing for the different approximations and  $z$  parameters. For the  $\alpha$  (blue) and  $\beta$  (green) orbits, the absolute numbers of the calculated dHvA frequencies change somewhat for the different  $z$ , being off from the experimental data for all three approximations, but the angular dependences are robust and agree with experiment. These two Fermi surfaces account for most of the experimentally observed dHvA data.

Further, there are clear dHvA signals for small angles (close to [001]) observed (see Ref. [31] for original data) that can nicely be attributed to the  $\gamma$  (red) or  $\delta$  (purple) sheets. Clearly, the dHvA frequencies  $\gamma_1$  at around 10 kT can only be attributed to the outer circumference of the pillow or donut. The low frequencies at about 370 T, however, may either be caused by the small spherical (purple) sheet with orbit  $\delta$  or by the hole of the (red) donut-like sheet for small  $z$  with orbit  $\gamma_4$ . These low frequencies, however, are detected only for a narrow angular range that would not be expected for the spherical Fermi surface ( $\delta$ ) orbit. A closed  $\gamma_4$  orbit, on the other hand, exists only close to [001]. Consequently, our data agree best with the calculations using LDA with optimized  $z$ .

In a next step, we now consider the influence of the La  $4f$  states on the calculated band-structure results. It is known that DFT calculations overestimate the hybridization of the  $4f$  states due to the underestimated

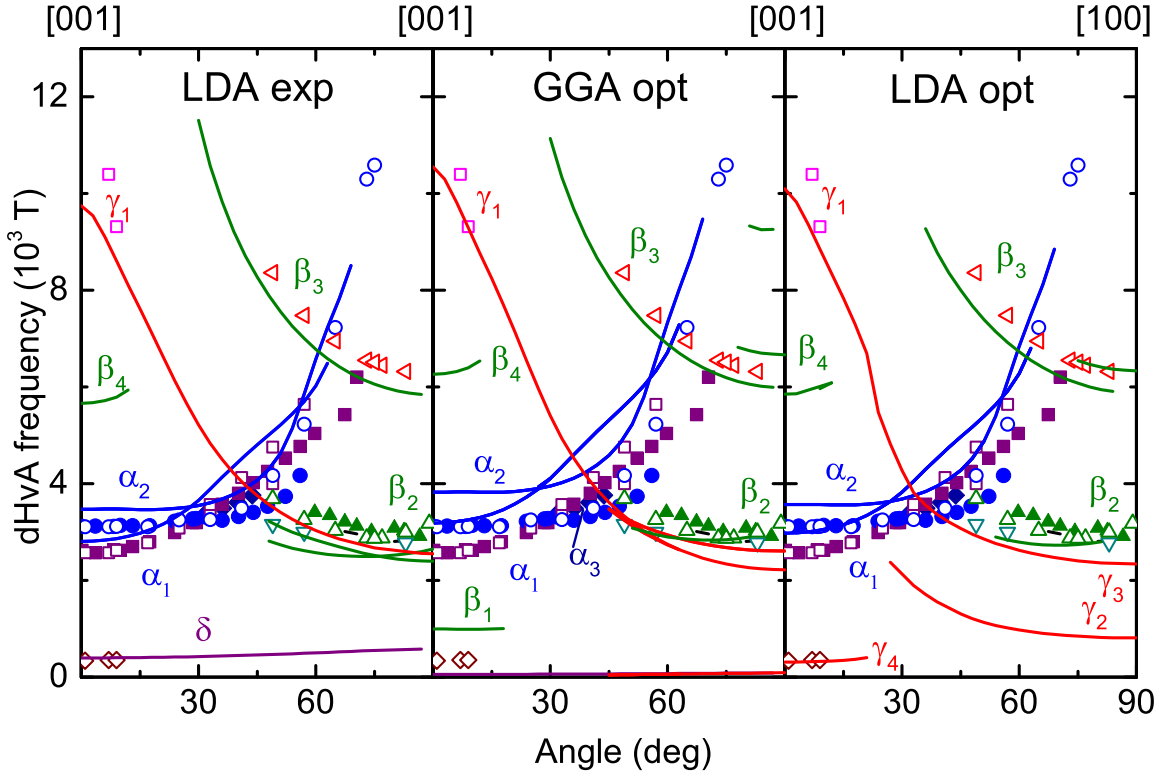


**Figure 4.** Angular dependence of the measured (symbols) and calculated (lines) dHvA frequencies estimated with different  $z$  parameters as explained in Fig. 2. The colors of the lines correspond to the colors of the Fermi surfaces shown in Fig. 3.

Coulomb repulsion in the rather localized  $4f$  orbitals, resulting in an energy too low for the unoccupied  $4f$  states shifting them too close to the Fermi energy. Experimentally, the unoccupied La  $4f$  peak is centered around 5 eV [41, 42], about 2.5 eV higher than in our calculation (see Fig. 5b).

Therefore we performed a so-called open-core calculation (ocore) where modifying the basis set of La manually moves the  $4f$  states into the core states [37] to study possible effects on the band structure and DOS. The result of this calculation is shown for the band structure and DOS in Fig. 5.

For the following calculations we fixed the P position to the optimum value using LDA, namely  $z = 0.3477$  [38]. For this

approximation, discussed above,  $\sim 3.5\%$  of the DOS at  $E_F$  originates from the La  $4f$  states.

Although the DOS at  $E_F$  changes only slightly, some noticeable modifications of the band structure occur [Fig. 5(a)]. These are rather pronounced between  $\Gamma$  and  $X$ , where the bands shift downward with decreasing  $4f$ -state fraction, whereas the bands shift upward around  $Z$  and close to  $E_F$ . Removing the  $4f$  states from the valence states, therefore, does not correspond to a rigid band shift of the Fermi energy.

The band shifts at  $Z$  are small, only up to about 0.1 eV. Nevertheless, this is sufficient to change the Fermi-surface topology of the (red) donut-like sheet (Fig. 6). As observed before

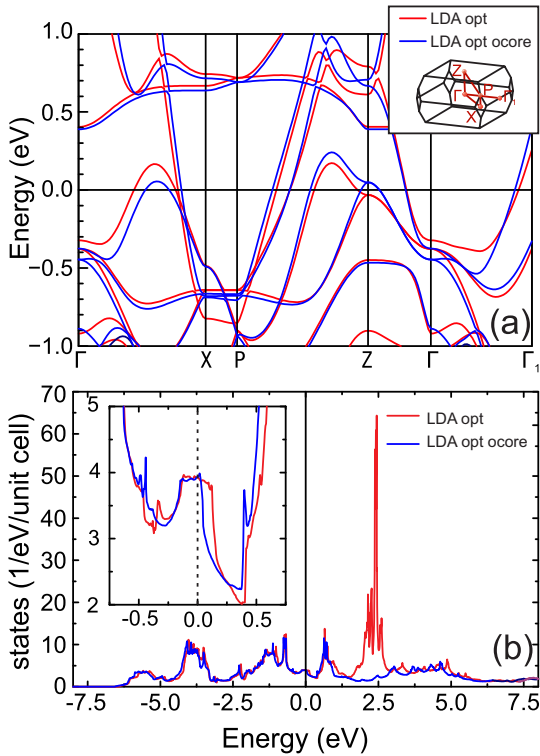


**Figure 5.** Band structure (a) and density of states (b) of  $\text{LaFe}_2\text{P}_2$ . The colors depict calculations using different treatments of the La  $4f$  states starting with (red) the optimized LDA result as shown already in Fig. 2. The open-core approximation calculation is shown in blue. The inset in (b) shows an enlargement of the density of states close to  $E_F = 0$ .

for the optimum  $z$  (Fig. 3), the green and blue Fermi-surface sheets change only their sizes but not their topologies. The red sheet, however, is modified considerably. For the open-core approximation, the hole vanishes leading to the reappearance of the pillow-like sheet and the fourth band of spherical shape. This as well leads to the vanishing of the  $\gamma_4$  and the appearance of the  $\delta$  orbit (Fig. 6).

When comparing the calculated extremal orbits with the dHvA results (Fig. 7), reasonable agreements for all treatments are found. However, best agreement appears to be obtained for the LDA open-core calculation. For all experimental dHvA data,

this approximation gives, besides the correct angular dependences, almost perfectly fitting absolute values for the dHvA frequencies. However, this calculation predicts as well a  $\delta$  frequency from a small sphere around  $Z$  that should be visible for all angles. Very close to the  $\delta$  another,  $\beta_1$ , frequency from the green Fermi-surface sheet is predicted. This latter orbit (Fig. 6) fits well with the experimentally observed data. It remains then, however, a puzzle why no signs of the  $\delta$  orbit are found in experiment. Possible reasons for that might be a high scattering rate (and Dingle temperature) for this orbit or an unfavorable curvature factor. In addition, the torque method is not very sensitive to such an isotropic, especially spherical Fermi surface. Further, since the orbit is just on the verge of existence, the “real” frequency might be somewhat smaller leading to a very slow dHvA oscillation that would be difficult to detect in the magnetization background. Anyway, besides these unsolved details of the possible existence of a fourth Fermi-surface sheet and the corresponding pillow or donut shape of the (red) sheet the quasi-two-dimensional (blue) and multiconnected (green) Fermi surfaces are nicely confirmed experimentally.

#### 4. Conclusion & Summary

We studied in detail the influence of the chosen exchange and correlation-potential  $V_{xc}$  approximations as well as the treatment of the  $4f$  states on the calculated band structure and  $z$  parameter in  $\text{LaFe}_2\text{P}_2$  and compared the results to experimental dHvA data. Since this compound shows no magnetic order it is well suited for such an investigation. Using the same structural input with different  $V_{xc}$  results, within the error bars, in the same Fermi-surface cross-sections. In contrast we

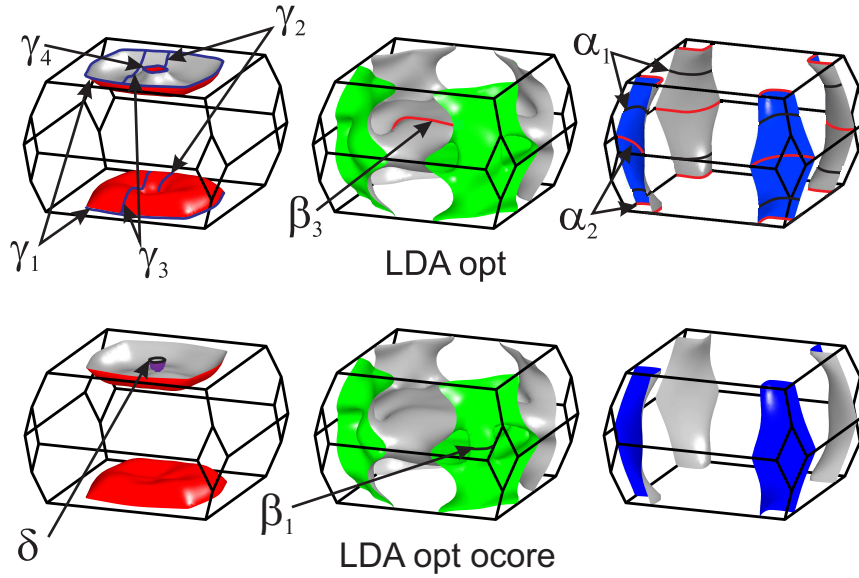


**Figure 6.** Calculated Fermi surfaces of  $\text{LaFe}_2\text{P}_2$  estimated by use of different treatments of the La 4*f* states as explained in Fig. 5. Some of the dHvA orbits are depicted by solid lines and labeled (see Fig. 7).

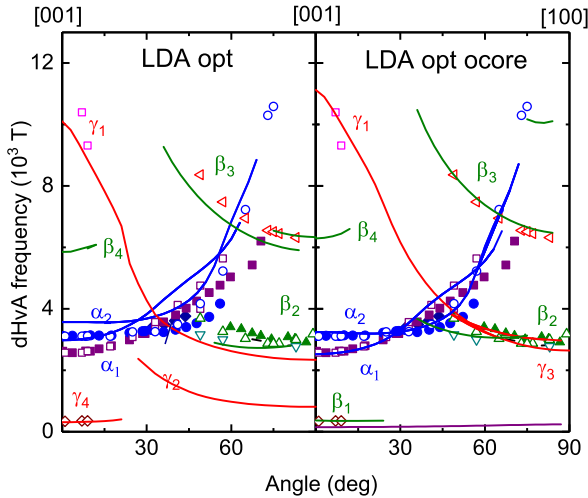


**Figure 7.** Angular dependence of the measured (symbols) and calculated (lines) dHvA frequencies estimated by use of different treatments of the La 4*f* states as explained in Fig. 5 and in the text.

found significant changes of the calculated  $z$  parameter when using different  $V_{xc}$ . This is observed as well for other 122 compounds, however, not always with such clear topology changes of the Fermi surface. For example,

for  $\text{BaIr}_2\text{P}_2$  the Fermi surface changes only marginally[39]. Although the calculated DOS at  $E_F$  has only about 3.5% 4*f* contribution in LDA removing the states leads to topological changes of the Fermi surface further improving the calculated result to a very good agreement with the experiment. In conclusion, our study shows that reliable low temperature structure data and a proper treatment of the formally unoccupied La 4*f* states is essential in order to have good agreement with the experiment.

## Acknowledgments

We acknowledge support from HLD at HZDR and LNCMI, members of the European Magnetic Field Laboratory (EMFL), and the Deutsche Forschungsgemeinschaft (SPP 1458).

## 5. References

- [1] D. Shoenberg, *Magnetic Oscillations in Metals* (Cambridge University Press, Cambridge 1984).
- [2] Y. Kamihara, H. Hiramsatsu, M. Hirano, R.

- Kawamura, H. Yanagi, T. Kamiya, and H. Hosono, *J. Am. Chem. Soc.* **128**, 10012 (2006).
- [3] T. Watanabe, H. Yanagi, T. Kamiya, Y. Kamihara, H. Hiramatsu, M. Hirano, and H. Hosono, *Inorg. Chem.* **46**, 7719 (2007).
- [4] Y. Kamihara, T. Watanabe, M. Hirano, and H. Hosono, *J. Am. Chem. Soc.* **130**, 3296 (2008).
- [5] S. Lebègue, *Phys. Rev. B* **75**, 035110 (2007).
- [6] D. J. Singh and M.-H. Du, *Phys. Rev. Lett.* **100**, 237003 (2008).
- [7] L. Boeri, O. V. Dolgov, and A. A. Golubov, *Phys. Rev. Lett.* **101**, 026403 (2008).
- [8] F. Ma and Z.-Y. Lu, *Phys. Rev. B* **78**, 033111 (2008).
- [9] I. I. Mazin, D. J. Singh, M. D. Johannes, and M. H. Du, *Phys. Rev. Lett.* **101**, 057003 (2008).
- [10] K. Kuroki, S. Onari, R. Arita, H. Usui, Y. Tanaka, H. Kontani, and H. Aoki, *Phys. Rev. Lett.* **101**, 087004 (2008).
- [11] M. M. Korshunov and I. Eremin, *Phys. Rev. B* **78**, 140509(R) (2008).
- [12] A. V. Chubukov, D. V. Efremov, and I. Eremin, *Phys. Rev. B* **78**, 134512 (2008).
- [13] V. Stanev, J. Kang, and Z. Tesanovic, *Phys. Rev. B* **78**, 184509 (2008).
- [14] Y. Ran, F. Wang, H. Zhai, A. Vishwanath, and D.-H. Lee, *Phys. Rev. B* **79**, 014505 (2009).
- [15] V. Cvetkovic and Z. Tesanovic, *EPL* **85**, 37002 (2009).
- [16] I. I. Mazin, *Nature (London)* **464**, 183 (2010).
- [17] C. Liu, G. D. Samolyuk, Y. Lee, N. Ni, T. Kondo, A. F. Santander-Syro, S. L. Bud'ko, J. L. McChesney, E. Rotenberg, T. Valla, A. V. Fedorov, P. C. Canfield, B. N. Harmon, and A. Kaminski, *Phys. Rev. Lett.* **101**, 177005 (2008).
- [18] L. X. Yang, Y. Zhang, H. W. Ou, J. F. Zhao, D. W. Shen, B. Zhou, J. Wei, F. Chen, M. Xu, C. He, Y. Chen, Z. D. Wang, X. F. Wang, T. Wu, G. Wu, X. H. Chen, M. Arita, K. Shimada, M. Taniguchi, Z. Y. Lu, T. Xiang, and D. L. Feng, *Phys. Rev. Lett.* **102**, 107002 (2009).
- [19] A. I. Coldea, J. D. Fletcher, A. Carrington, J. G. Analytis, A. F. Bangura, J.-H. Chu, A. S. Erickson, I. R. Fisher, N. E. Hussey, and R. D. McDonald, *Phys. Rev. Lett.* **101**, 216402 (2008).
- [20] A. Carrington, A. I. Coldea, J. D. Fletcher, N. E. Hussey, C. M. J. Andrew, A. F. Bangura, J. G. Analytis, J.-H. Chu, A. S. Erickson, I. R. Fisher, and R. D. McDonald, *Physica C* **469**, 459 (2009).
- [21] H. Muranaka, Y. Doi, K. Katayama, H. Sugawara, R. Settai, F. Honda, T. D. Matsuda, Y. Haga, H. Yamagami, and Y. Onuki, *J. Phys. Soc. Jpn.* **78**, 053705 (2009).
- [22] S. E. Sebastian, J. Gillett, N. Harrison, P. H. C. Lau, D. J. Singh, C. H. Mielke, and G. G. Lonzarich, *J. Phys.: Condens. Matter* **20**, 422203 (2008).
- [23] N. Harrison, R. D. McDonald, C. H. Mielke, E. D. Bauer, F. Ronning, and J. D. Thompson, *J. Phys.: Condens. Matter* **21**, 322202 (2009).
- [24] A. E. Coldea, C. M. J. Andrew, J. G. Analytis, R. D. McDonald, A. F. Bangura, J.-H. Chu, I. R. Fisher, and A. Carrington, *Phys. Rev. Lett.* **103**, 026404 (2009).
- [25] J. G. Analytis, C. M. J. Andrew, A. I. Coldea, A. McCollam, J.-H. Chu, R. D. McDonald, I. R. Fisher, and A. Carrington, *Phys. Rev. Lett.* **103**, 076401 (2009).
- [26] J. G. Analytis, R. D. McDonald, J.-H. Chu, S. C. Riggs, A. F. Bangura, C. Kucharczyk, M. Johannes, and I. R. Fisher, *Phys. Rev. B* **80**, 064507 (2009).
- [27] A. Carrington, *Rep. Prog. Phys.* **74**, 124507 (2011).
- [28] A. I. Coldea, D. Braithwaite, and A. Carrington, *C. R. Physique* **14**, 94 (2013).
- [29] R. Mittal, S. K. Mishra, S. L. Chaplot, S. V. Ovsyannikov, E. Greenberg, D. M. Trots, L. Dubrovinsky, Y. Su, Th. Brueckel, S. Matsuishi, H. Hosono, and G. Garbarino, *Phys. Rev. B* **83**, 054503 (2011).
- [30] D. Kasinathan, M. Schmitt, K. Koepf, A. Ormeci, K. Meier, U. Schwarz, M. Hanfland, Ch. Geibel, Y. Grin, A. Leithe-Jasper, and H. Rosner, *Phys. Rev. B* **84**, 054509 (2011).
- [31] S. Blackburn, B. Prévost, M. Bartkowiak, O. Ignatchik, A. Polyakov, T. Förster, M. Côté, G. Seyfarth, C. Capan, Z. Fisk, R. G. Goodrich, I. Sheikin, H. Rosner, A. D. Bianchi, and J. Wosnitza, *Phys. Rev. B* **89**, 220505(R) (2014).
- [32] K. Koepf and H. Eschrig, *Phys. Rev. B* **59**, 1743 (1999).
- [33] J. P. Perdew and Y. Wang, *Phys. Rev. B* **45**, 13244 (1992).
- [34] J. P. Perdew, K. Burke, and M. Ernzerhof, *Phys. Rev. Lett.* **77**, 3865 (1996).
- [35] M. Reehuis and W. Jeitschko, *J. Phys. Chem. Solids* **51**, 961 (1990).
- [36] W. Jeitschko, U. Meisen, M. H. Müller, and M. Reehuis, *Z. Anorg. Allg. Chem.* **527**, 73 (1985).

- [37] The used base for La is for the core:  $1s\ 2s\ 2p\ 3s\ 3p\ 3d\ 4s\ 4p\ 4d\ 4f$  and for the valence electrons:  $5s\ 5p\ 6s\ 5d\ 6p$ . The remaining basis set was not modified.
- [38] We did not find any influence of the  $4f$ -state treatment on the optimum  $z$  position.
- [39] T. Förster, B. Bergk, O. Ignatchik, M. Bartkowiak, S. Blackburn, M. Côté, G. Seyfarth, N. Berry, Z. Fisk, I. Sheikin, A. D. Bianchi, and J. Wosnitza, *Phys. Rev. B* **92**, 134518 (2015).
- [40] K. Lejaeghere, et al., *Science* **351**, 6280 (2016).
- [41] A. V. Fedorov, C. Laubschat, K. Starke, E. Weschke, K.-U. Barholz, and G. Kaindl, *Phys. Rev. Lett.* **70**, 1719 (1993).
- [42] J. K. Lang, Y. Baer, and P.A. Cox, *J. Phys. F: Metal Physics* **11**, 121 (1981).
- [43] K. Götze, I. Kraft, J.Klotz. et al. to be published.